Published in final edited form as:
Anal Chem. 2010 August 1; 82(15): 6704–6711. doi:10.1021/ac101461x.

Microfluidic System for Generation of Sinusoidal Glucose Waveforms for Entrainment of Islets of Langerhans

Xinyu Zhang[†], **Alix Grimley**[†], **Richard Bertram**[‡], and **Michael G. Roper**[†,*]

[†]Department of Chemistry and Biochemistry and Program in Molecular Biophysics, Florida State University, Tallahassee, FL

[‡]Department of Mathematics and Programs in Neuroscience and Molecular Biophysics, Florida State University, Tallahassee, FL

Abstract

A microfluidic system was developed to produce sinusoidal waveforms of glucose to entrain oscillations of intracellular [Ca^{2+}] in islets of Langerhans. The work described is an improvement to a previously reported device where two pneumatic pumps delivered pulses of glucose and buffer to a mixing channel. The mixing channel acted as a low pass filter to attenuate these pulses to produce the desired final concentration. Improvements to the current device included increasing the average pumping frequency from 0.83 Hz to 3.33 Hz by modifying the on-chip valves to minimize adhesion between the PDMS and glass within the valve. The cutoff frequency of the device was increased from 0.026 Hz to 0.061 Hz for sinusoidal fluorescein waves by shortening the length of the mixing channel to 3.3 cm. The value of the cutoff frequency was chosen between the average pumping frequency and the low frequency (~0.0056 Hz) glucose waves that were needed to entrain islets of Langerhans. In this way, the pulses from the pumps were attenuated greatly, but the low frequency glucose waves were not. Using this microfluidic system, a total flow rate of 1.5 ± 0.1 μL min^{-1} was generated and used to deliver sinusoidal waves of glucose concentration with a median value of 11 mM and amplitude of 1 mM to a chamber that contained an islet of Langerhans loaded with the Ca^{2+}-sensitive fluorophore, indo-1. Entrainment of the islets was demonstrated by pacing the rhythm of intracellular [Ca^{2+}] oscillations to oscillatory glucose levels produced by the device. The system should be applicable to a wide range of cell types to aid in understanding cellular responses to dynamically changing stimuli.

Keywords

microfluidic; pumping; temporal; gradient; islet; entrainment

Introduction

Synchronized insulin release from a large number of islets of Langerhans in the pancreas (~1×10^6 islets in human pancreas) results in oscillatory insulin levels in the blood. Insulin-dependent tissues are more sensitive to oscillatory insulin levels than to constant levels, and impaired insulin oscillations are a characteristic of type II diabetics.[1-7] Understanding the mechanisms involved in synchronization of the large numbers of islets in the pancreas is therefore of utmost importance.

[*]Address Correspondence to: Dr. Michael G. Roper, Department of Chemistry and Biochemistry, Florida State University, 95 Chieftain Way, Dittmer Building, Tallahassee, FL 32306, Ph 850-644-1846, Fx 850-644-8281, roper@chem.fsu.edu.

One hypothesis of how islets synchronize is through a liver-pancreas feedback loop.[8-10] As blood glucose levels rise, glucose-stimulated insulin release from islets is increased, which in turn, facilitates glucose consumption in the liver and other insulin-dependent tissues. Consequently, the glucose level lowers, resulting in decreased insulin release from the pancreas as well as decreased glucose consumption. This lowering of insulin levels then enables glucose levels to rise again, initiating another cycle of insulin release and a subsequent decline in glucose levels. As all islets sense blood glucose levels, these oscillatory blood glucose levels would induce synchronized and oscillatory insulin release from the pancreas. There is evidence for this hypothesis, as glucose levels are known to oscillate *in vivo* with periods similar to insulin secretory oscillations.[8,11,12] A mathematical model has shown that a liver-pancreas interaction can result in synchronization of insulin release from a large number of islets.[10] The first step in experimentally verifying this hypothesis is to determine if an oscillatory glucose stimulus can entrain the islet response. Entrainment is defined here as the control and regulation of the oscillatory nature of islets to an external forcing signal.[13]

There is conflicting evidence on the entrainability of islets of Langerhans. Several reports have indicated that insulin released from single islets is entrained to periodic glucose exposure.[9,14] Whereas others have shown no change in insulin secretory oscillations with periodic glucose pulses[13], or entrainment of intracellular $[Ca^{2+}]$ ($[Ca^{2+}]_i$) was only observed with pulses of high glucose concentration[15]. To aid in further studies of islet entrainment, it would be beneficial to have a system that could produce accurate and precise oscillatory concentrations of glucose in a perfusion system for delivery to islets of Langerhans.

Recently, several examples of microfluidic devices used for cellular perfusion have been described.[16-20] As dispersive channels act as low pass filters[21,22], output waveforms generated within a microfluidic chip need to be within the bandwidth of the device, yet still provide complete mixing of reagents prior to delivery to the cell chamber. In previous work, a simple microfluidic device was developed to produce a series of time-dependent concentrations of an analyte.[23] This device was applied to stimulate islets of Langerhans with step changes of glucose concentration to initiate changes in $[Ca^{2+}]_i$. A cursory examination of the bandwidth of the device was performed; however, the reproducibility of higher frequency waves was low and frequencies higher than 0.0025 Hz were attenuated. As frequencies between 0.0033 and 0.0056 Hz are needed to test the entrainment of islets, the previous system would not be suitable for this task.

In this report, previously developed theory[21,22] was used to modify the chip design to ensure that the cutoff frequency of the device was lower than the pumping frequency, yet higher than the frequencies of the glucose waveforms needed to entrain islets. This cutoff frequency was chosen to attenuate the pulses from the pumps to produce a well-mixed desired final concentration, but not attenuate the output glucose waveforms. The cutoff frequency was increased from the previous 0.026 Hz to 0.061 Hz by two major modifications: modifying the pneumatic valves to raise the average pumping frequency from 0.83 Hz to 3.33 Hz and shortening the mixing channel from 12 cm to 3.3 cm. This newly developed device was used to entrain $[Ca^{2+}]_i$ oscillations within islets to sinusoidal glucose waveforms.

Theory

As has been well described, dispersive microfluidic channels act as low pass filters to periodic inputs.[21,22,24,25] As shown before[21,22], the amount of attenuation of an output wave is dependent on the input frequency (f) and the length of the channel (L). The ratio of the output waveform, $C_{out}(f,L)$, to the input waveform, $C_{in}(f,0)$, can be approximated by:

$$\left\|\frac{C_{out}(f,L)}{C_{in}(f,0)}\right\| \approx \exp\left(-\frac{f^2}{f_C^2}\right) \quad (1)$$

where f_C is the cut-off frequency of the low pass filter. As indicated by equation 1, if the input frequency is higher than the cutoff frequency, the periodic input signal will be attenuated. As will be shown below, the high frequency pulses from the two on-chip pumps were used to generate low frequency glucose waveforms. Figure 1A shows a series of high frequency pulses, where each pulse indicates when an analyte plug was delivered to the mixing channel using the optimal pumping system described in this report (3.33 Hz). Since these high frequency pulses of analyte are attenuated as they travel through the mixing channel, the final concentration is proportional to the pulse density. Figure 1B shows the amount of attenuation of a microfluidic device using a cutoff frequency of 0.061 Hz modeled with equation 1. The low frequencies needed to test the entrainment of islets is shown by shaded region 1, and the high frequencies used for pumping are highlighted by shaded region 2. After passing the pulses shown in Figure 1A through the microfluidic device with the characteristics of the low pass filter shown in Figure 1B, the result is shown in Figure 1C where the high frequency pulses from the pumps have been attenuated while a 0.009 Hz wave remains. As can be seen, the position of the cutoff frequency is critical in achieving the desired experimental results.

The cutoff frequency can be approximated by[21,22]:

$$f_C \approx \frac{1}{2\pi}\left[\frac{V^3}{DL}\right]^{1/2} \quad (2)$$

where V is the average linear flow velocity through the mixing channel and D is the dispersion adjusted diffusion constant. In the previous report, the cutoff frequency of fluorescein waves was 0.026 Hz with waveforms attenuated above frequencies of 0.0025 Hz, too slow to entrain islets. To increase the cutoff frequency, V could be increased or L decreased. As will be described below, the changes to velocity were limited by the total pumping frequency and pneumatic valve size. Therefore, L was optimized to produce the filter characteristics that would attenuate high frequencies from the pumps, but not the low frequencies used to entrain islets.

Experimental

Chemicals and Reagents

HNO_3, $CaCl_2$, NaOH, and NaCl were purchased from EMD Chemicals, Inc. (Gibbstown, NJ). Polydimethylsiloxane (PDMS) was from Rogers Corporation (Carol Stream, IL). $MgCl_2$, HF and Cosmic Calf Serum (CCS) were from Fisher Scientific (Pittsburgh, PA). KCl, fluorescein, tricine, dimethyl sulfoxide (DMSO) and Type XI collagenase were from Sigma (St. Louis, MO). Indo-1 acetoxymethyl ester (indo-1 AM), Pluronic F-127, RPMI 1640, and penicillin-streptomycin were from Invitrogen (Carlsbad, CA). All solutions were made with Milli-Q (Millipore, Bedford, MA) 18 MΩ·cm deionized water.

All solutions used in the microfluidic device were made with a buffer composed of 2.4 mM $CaCl_2$, 125 mM NaCl, 1.2 mM $MgCl_2$, 5.9 mM KCl and 25 mM tricine, and made to pH 7.4 with NaOH. This buffer was supplemented with either fluorescein or glucose when characterizing pumps or performing islet measurements, respectively. Accordingly, the

solutions used in solvent and analyte pumps, respectively, were: buffer and 100 μM fluorescein, or 3 mM and 13 mM glucose.

Chip Design and Pumping Program

The device was fabricated as previously described[23] with the following modifications for increased pumping frequencies. The fluidic channel dimensions in the pumping region were 220 μm × 50 μm (width × depth). Within each valve, a 20 μm gap was used to separate the fluidic channels. The valve seats were etched to 1.10 mm × 0.35 mm × 50 μm (length × width × depth). The fluidic channels from the 3rd valves to 2 mm after the junction of the two pumping channels were 80 × 30 μm (width × depth). To shorten the length of the plugs in the longitudinal direction[24], the remaining 31 mm of the mixing channel was 220 × 90 μm (width × depth).

A pump cycle was composed of 5 steps, the first 4 steps having times of 40, 30, 40, and 40 ms, respectively. Since the sum of these 4 steps was 150 ms, the total number of pump cycles of identical volume that could be performed by a single pump in one minute was 400. The distribution of these 400 pump cycles to the two pumps dictated the final dilution and was performed by determining an idle time as the 5th step in the valving sequence. Equations (3) and (4) give the idle time for a designated concentration.

$$IT_{PumpA} = 0.15\left(\frac{1 - x_A}{x_A}\right) \qquad 0 < x_A < 1 \tag{3}$$

$$IT_{PumpB} = 0.15\left(\frac{x_A}{1 - x_A}\right) \qquad 0 < x_A < 1 \tag{4}$$

where $IT_{Pump\ A}$ and $IT_{Pump\ B}$ were the idle times for pumps A and B, respectively, and x_A was the final dilution of analyte from pump A. The value of x_A was determined manually or was automatically generated and entered into a program (LabView, National Instruments, Austin, TX). The program was used to calculate and control the timing and to actuate solenoid valves (Model A00SC232P, Parker Hannifin Corp., Cleveland, OH) via a PCI-6220 data acquisition card (National Instruments). The solenoid valves directed air or vacuum to close or open the microfluidic valve seats. In all experiments, a thermofoil and thermocouple sensor (Omega Engineering, Inc., Stamford, Connecticut) were attached to the microfluidic chip to maintain the temperature of the device at 37 °C.

Isolation of Islets of Langerhans

Islets of Langerhans were collected as previously described.[23] For $[Ca^{2+}]_i$ monitoring, 1.0 μL of 5.0 mM indo-1 AM in DMSO and 1.0 μL Pluronic F-127 in DMSO were mixed and transferred into 2 mL RPMI with 11 mM glucose to form a final indo-1 AM concentration of 2.5 μM. Each islet was placed in this solution and incubated at 37 °C, 5% CO_2 for 45 min. After incubation, the islet was transferred to the cell chamber in the microfluidic device and washed by perfusion with 3 mM glucose prior to monitoring $[Ca^{2+}]_i$.

Detection

For waveform characterization, fluorescein fluorescence was monitored at the end of the mixing channel using a Nikon TS100F microscope. Fluorescence from indo-1 was monitored using a Nikon Eclipse Ti microscope and a broadband lamp (Lambda XL, Sutter

Instrument, Novato, CA). The lamp was integrated with a shutter (Sutter), which opened 2 ms every 5 s to reduce photobleaching of indo-1. Excitation light from the lamp was sent through an excitation filter (XF1004, Omega Optical, Brattleboro, VT) and the 355 nm light was made incident on a multi-band dichroic cube (XF2003, Omega Optical). The excitation light was focused onto the islet through a 40×, 0.6 NA objective, and the emission was collected by the same objective. The collected emission was sent through the multi-band cube and entered into a microscope photometer (Photon Technology International, Inc., Birmingham, NJ) containing a spatial filter. After passing through the spatial filter, the emission was split into 405 nm and 485 nm via a second dichroic mirror (XF2006, Omega Optical). Bandpass filters (XF3004 and XF3005, Omega Optical) were used in front of two photomultiplier tubes to minimize crosstalk between the emission channels. All indo-1 fluorescence measurements are shown as the ratio of the fluorescence from the two emission channels which is proportional to $[Ca^{2+}]_i$.[26]

Results and Discussion

As shown in Figure 2A, pumps A and B, each composed of three pneumatic valves, delivered analyte and buffer into the mixing channel. Ideally, the flow from each of these pumps would be continuous and the ratio of the widths of the two fluids entering the mixing channel would dictate the final concentration. Instead, a pulse of either buffer or analyte was delivered to the mixing channel in each pumping cycle. In this way, the final concentration of analyte was produced by longitudinal mixing of the buffer and analyte pulses within a given period of time. This device is similar to a microfluidic device previously described for producing output concentrations using pulse code modulation.[21,27] The improvements to the device were driven by the theory outlined above and consisted of two main features: increasing the pumping and cutoff frequency. As shown in equation 2, the cutoff frequency depends on the linear flow rate through the device, which depends on the valve size and pumping rate.[28] Due to this dependence, the pumping frequency was first increased followed by optimization of the mixing channel length to make the final adjustments to the cutoff frequency.

Increasing the pumping frequency

In the previous iteration of the device, the average pumping frequency was 0.83 Hz. An attempt was made to increase this frequency, but as the pump frequency rose, the opening and closing time of each valve was reduced, resulting in incomplete opening and closing of the valves. It was observed that the amount of time needed to open and close the valve was limited by the time to break the adhesion between the glass and PDMS within the valve. To raise the pumping frequency, the contact area between the PDMS layer and the glass was decreased.

The reduction in contact area was accomplished by varying the sizes of the gap between the fluidic channel and the valve seat. It was found that a 20 μm gap in the fluidic channels and a narrow but deep valve seat (0.35 mm × 50 μm, width × depth) allowed for rapid actuation of the valve. As shown in Figure 2B, the narrow valve seat and short distance between the fluidic channels reduced the area of PDMS attached to the glass when the valve was closed, and the narrow and deep valve seat avoided contact of PDMS with the bottom glass piece when the valve was opened. With these modifications, the pumps were operated at 8.35, 6.65, 5.00, and 3.33 Hz and the pumping monitored. 3.33 Hz was selected as the optimum since the valves did not open or close sufficiently at the higher frequencies, which resulted in irreproducible flow rates, incorrect dilutions, and distorted waveforms. However, even with the increased pumping rate, the flow rate generated was 1.5 μL/min (see below), which was similar to the previous device and found ideal for quickly flushing out the 200 nL cell chamber while minimizing shear stress on the islet.

Increasing the cutoff frequency

The frequency of the waveforms needed to entrain islets dictated the required cutoff frequency of the microfluidic chip. As shown below, islets were entrained with glucose waveforms with frequencies between 0.0033 and 0.0056 Hz. Therefore, the cutoff frequency needed to be higher than 0.0056 Hz to ensure the amplitude attenuation at these frequencies was minimal. We set the cutoff frequency to be not less than 0.05 Hz. In our previous device, the cutoff frequency was 0.025 Hz with significant attenuation at frequencies too low to entrain islets.

As shown in equation 2 and described earlier, the length of the mixing channel was altered to vary the cutoff frequency. To determine the optimum length, a series of fluorescein concentrations were produced with the on-chip pumps. The RSD of the fluorescence signal was measured at various mixing channel lengths. At short mixing channel lengths, the RSD was large (> 50%) due to the large signal variation from the plugs of fluorescein and buffer that had not completely mixed. This situation is analogous to a cutoff frequency close to the pumping frequency. As the detection point was moved down the mixing channel, the cutoff frequency was decreased. The optimum mixing channel length was chosen as the distance where the RSD was smaller than 2% for a constant output fluorescein concentration. At this point, the cutoff frequency was deemed low enough to attenuate the high frequency noise from the fluorescein and buffer plugs, yet high enough to not attenuate glucose waveforms for islet entrainment. The longest mixing distance necessary to achieve a 2% RSD was 3.3 cm. Shorter mixing distances will increase the bandwidth of glucose waveforms, but at the expense of high RSDs leading to low signal to noise ratios.

Using the design modifications outlined above, a calibration curve was produced by outputting a series of fluorescein concentrations. A linear curve of PMT voltage (V) vs. fluorescein concentration (μM) was produced with the equation for the best fit line as, $y = 0.067x + 0.072$ with an r^2 value of 0.999. The flow rate, measured as previously reported[23], was 1.5 ± 0.1 μL/min, or 3.8 ± 0.3 nL/cycle over all dilution percentages tested.

Rapid sine waves

Sinusoidal waves of fluorescein concentration with periods of 0.009 Hz, 0.018 Hz, 0.030 Hz, 0.045 Hz, 0.060 Hz, and 0.090 Hz were produced with a median value of 50 μM (Figure 3). For each frequency, at least 4 periods were produced at amplitudes of 40, 30, 20, and 10 μM. The dashed horizontal lines in Figure 3 indicate the PMT values corresponding to these amplitudes as determined by an on-line calibration. To quantitatively evaluate the attenuation, the ratio of the output amplitude to the input amplitude was plotted *versus* frequency of the input waveforms. All plots are displayed in Figure 4, except the 0.090 Hz due to the poor reproducibility of the waveform. Sine waves with a period of 0.009 Hz produced waveforms with 2.1% attenuation, whereas the other waves were attenuated to higher degrees, as expected for a low pass filter.

Using the current system, the cutoff frequency for fluorescein, as defined in equations 1 and 2, was 0.061 Hz as compared to 0.026 Hz with the previously reported design. The dashed line in Figure 4 is the theoretical attenuation of a low pass filter found by equation 1 using a value of 0.061 Hz as f_C. As can be seen, there was excellent agreement between the theoretical and measured attenuation. It should be noted that sine waves generated with frequencies lower than 0.011 Hz had less than 3% attenuation, whereas in the previous system the frequency had to be lower than 0.0025 Hz to achieve this level of attenuation.

Since the dispersion-adjusted diffusion coefficient used in equation 2 is inversely proportional to the intrinsic diffusion coefficient[22], the f_c of glucose would be approximately 0.076 Hz using an intrinsic diffusion coefficient of 6.65×10^{-6} cm^2/s.[29] As the f_c of glucose

was higher than the f_c of fluorescein, there should be less attenuation of the glucose waveforms than the fluorescein waveforms. Since a typical frequency sufficient to entrain islets was 0.0056 Hz (see below), the current device was readily able to generate these glucose waves with little attenuation.

As shown in reference 28, increased valve sizes can increase flow rates, but at the expense of decreased pumping frequencies. In the future, the first step needed to increase the bandwidth of the device will be to produce higher pumping frequencies, which will allow a higher cutoff frequency to be selected. To produce higher pumping frequencies, other materials may be needed for the diaphragm to lessen the adhesion to the glass. For example, fluorinated polymers have been used with these valves[30]; however, the Young's modulus of PDMS is orders of magnitude lower than in these films, making PDMS more attractive for rapid pumping. A thinner piece of PDMS could be actuated faster, which may allow for faster pumping rates. The use of an all PDMS-based device with integrated valves can generate more rapid pumping frequencies[31], which may be an alternative to the current device. However, we believe that when the pumping frequency gets very high the flow will be continuous in nature, not pulsatile, which will lead to a different set of criteria for producing concentration gradients.

A major difference between our device and others that have used similar methods to produce on-chip dilutions, is that the valves in this report are used to produce the pulses into the mixing channel and also drive solution flow. Other reports have used off-chip methods to drive fluid flow and fewer valves to direct a pulse into a mixing channel.[21,27,32] Using these methods, the pulsing frequency should be much higher compared to the device reported here since fewer steps are needed to produce a pulse. Even with this limitation of the current device, output waveforms needed to test islet entrainment could be produced with minimal attenuation.

Entrainment of islets

After the above modifications were made to the microfluidic device to ensure that low frequency oscillations of glucose could be made with minimal attenuation, entrainment of islets was attempted. As shown below, stimulation of islets with a constant 11 mM glucose induced oscillations of $[Ca^{2+}]_i$ that had a frequency between 0.0033 and 0.0056 Hz. The origin of these slow $[Ca^{2+}]_i$ oscillations are not the subject of this manuscript, but have been attributed to oscillations in glycolysis.[33-35] Insulin release is known to follow $[Ca^{2+}]_i$ increases[36,37] and we used $[Ca^{2+}]_i$ as a marker of insulin release.

As shown in Figure 5A, experiments were initiated at a basal level of 3 mM glucose (red line) while $[Ca^{2+}]_i$ was monitored (black line). After a short period of time, the glucose concentration was increased to 11 mM, initiating $[Ca^{2+}]_i$ oscillations which had a frequency between 0.0033 and 0.0056 Hz. To entrain this oscillatory $[Ca^{2+}]_i$ response, in the middle of the 5th oscillation, the constant glucose concentration was changed to a sinusoidal waveform with a frequency determined from the average of the periods from the 3rd and 4th $[Ca^{2+}]_i$ oscillation and an amplitude of 1 mM.

To determine if the $[Ca^{2+}]_i$ responses were entrained to the forcing glucose signal, a phase offset ($\Delta\theta$) between each $[Ca^{2+}]_i$ oscillation and the glucose waves was measured. If the islets were entrained, the $[Ca^{2+}]_i$ oscillations would shift in time to the glucose waves. $\Delta\theta$ was found by measuring the difference in the start times of each glucose wave (t_g) and the closest $[Ca^{2+}]_i$ oscillation (t_c):

$$\Delta\theta = 360^\circ (t_c - t_g)/T \quad (5)$$

where T was the period of the glucose wave applied to the islet. Figure 5B details t_g and t_C for the first two glucose waves shown in Figure 5A. To compare how the $[Ca^{2+}]_i$ oscillations changed after applying the oscillatory glucose levels, the $[Ca^{2+}]_i$ oscillations during the stable 11 mM glucose were analyzed by supposing the oscillatory glucose waveform extended for the entire duration of the $[Ca^{2+}]_i$ trace.

Figure 5C shows how Δθ changed as a function of the number of glucose waves applied (N_g). The 5 traces shown were representative of all islets tested (n = 7 from 5 mice). The start of the first glucose sine wave was at $N_g = 0$, with negative values of N_g representing $[Ca^{2+}]_i$ oscillations prior to the onset of sinusoidal glucose pulses. As can be seen, prior to the onset of glucose waves ($N_g < 0$), there was a drift in Δθ for all islets. When the glucose wave was applied, Δθ shifted to a new value and remained relatively constant throughout the duration of the applied glucose waves. The shift in Δθ and its subsequent invariance are good indications that glucose waves entrained islet $[Ca^{2+}]_i$ oscillations.

For a control experiment, a similar analysis was made on islets that did not receive an oscillatory glucose input (n = 3). For purposes of analysis only, a sine wave with a period determined as described above was superimposed on the $[Ca^{2+}]_i$ trace and Δθ calculated. In contrast to the results seen when an oscillatory glucose concentration was applied, in all islets tested without a rhythmic glucose signal, Δθ varied throughout the experiment (one example shown in Figure 5C, open symbols).

180° Phase Shift

Although the change in Δθ did imply entrainment, a second type of experiment was performed wherein after the sine wave of glucose concentration had been applied for several periods, a 180° phase shift was inserted into the glucose waves (Figure 6). The reason for the 180° phase shift was to “unentrain” the islet and determine if it would become entrained again to the phase shifted glucose wave. If the islet was not entrained, the $[Ca^{2+}]_i$ oscillations would continue independent of the glucose waveform and the resulting trace of Δθ vs. N_g would show a jump of 180° after the glucose phase shift. However, if the islet was entrained to the glucose pulses, the $[Ca^{2+}]_i$ oscillations would need to reset to the new glucose wave to maintain a constant Δθ.

Shown in Figure 6A are two representative traces of the glucose phase shift experiment. The results of all 5 islets tested (from 4 mice) are quantified in Figure 6B and demonstrate that upon application of the glucose phase shift, the $[Ca^{2+}]_i$ oscillations quickly reset to maintain a constant Δθ before and after the phase shift occurred. This process can be observed in Figure 6A, where the $[Ca^{2+}]_i$ oscillation during the glucose phase shift expanded as compared to the other oscillations in the figures. The shift in Δθ upon initiation of the glucose waves (Figures 5 and 6), and the maintenance of a constant Δθ before and after a 180° glucose phase shift (Figure 6), provide further evidence that the islets were successfully entrained by the forcing glucose signal produced by the microfluidic device.

Conclusion

A simple microfluidic device was developed to generate glucose waveforms to test the entrainment of islets of Langerhans. The ability to increase the average pumping frequency from 0.83 Hz to 3.33 Hz and shortening of the mixing channel length increased the cutoff frequency to 0.061 Hz for fluorescein waves. The factor that limited the use of a higher

cutoff frequency was the pumping frequency. Although the opening and closing of the computer-controlled solenoid valves used to deliver air and vacuum to the microfluidic device have the ability to be operated at higher frequencies than what was used in these experiments, other alterations of the valve geometry or the use of a different material would be needed to increase the pumping rate.

The use of this device allowed examination of the entrainment of $[Ca^{2+}]_i$ oscillations in single islets of Langerhans to a sinusoidal glucose input. The analysis showed that the $[Ca^{2+}]_i$ oscillations were modified and regulated by the glucose waves, which provided the evidence that the $[Ca^{2+}]_i$ oscillations were entrained. This device should be applicable to further experiments investigating the oscillatory nature of islets of Langerhans. As this device is ideal for producing an oscillatory stimulation, it should also be applicable in investigating the frequency response of other cell types.[20,38,39]

In the future, the microfluidic device could be further developed for stimulating multiple islets simultaneously to provide a more high-throughput approach. Additional analyte channels could be added to extend the concentration range or achieve a multi-analyte perfusion system. In addition, a multi-analyte system could provide higher pumping frequency to further reduce amplitude attenuation and raise the frequency of output waveforms.

Acknowledgments

XYZ, AG, and MGR were funded from grants by the NIH (R01 DK080714) and the American Heart Association Greater Southeast affiliate. RB was supported by NSF grant DMS-0917664.

References

1. Weigle DS. Diabetes 1987;36:764–775. [PubMed: 3552804]
2. Matthews DR, Naylor BA, Jones RG, Ward GM, Turner RC. Diabetes 1983;32:617–621. [PubMed: 6134649]
3. Bratusch-Marrain PR, Komjati M, Waldhausl WK. Diabetes 1986;35:922–926. [PubMed: 3525288]
4. Komjati M, Bratusch-Marrain P, Waldhausl W. Endocrinology 1986;118:312–319. [PubMed: 3000741]
5. Paolisso G, Scheen AJ, Giugliano D, Sgambato S, Albert A, Varricchio M, D'Onofrio F, Lefebvre PJ. J Clin Endocrinol Metab 1991;72:607–615. [PubMed: 1997515]
6. Polonsky KS, Given BD, Hirsch LJ, Tillil H, Shapiro ET, Beebe C, Frank BH, Galloway JA, Van Cauter E. N Engl J Med 1988;318:1231–1239. [PubMed: 3283554]
7. O'Rahilly S, Turner RC, Matthews DR. N Engl J Med 1988;318:1225–1230. [PubMed: 3283553]
8. Lang DA, Matthews DR, Burnett M, Turner RC. Diabetes 1981;30:435–439. [PubMed: 7014311]
9. Chou HF, Ipp E. Diabetes 1990;39:112–117. [PubMed: 2210053]
10. Pedersen MG, Bertram R, Sherman A. Biophys J 2005;89:107–119. [PubMed: 15834002]
11. Lang DA, Matthews DR, Peto J, Turner RC. N Engl J Med 1979;301:1023–1027. [PubMed: 386121]
12. Mao CS, Berman N, Roberts K, Ipp E. Diabetes 1999;48:714–21. [PubMed: 10102686]
13. Ritzel RA, Veldhuis JD, Butler PC. Am J Physiol Endocrinol Metab 2006;290:E750–E756. [PubMed: 16278244]
14. Sturis J, Pugh WL, Tang JP, Ostrega DM, Polosnky JS, Polonsky KS. Am J Physiol 1994;267:E250–E259. [PubMed: 8074204]
15. Zarkovic M, Henquin JC. Am J Physiol Endocrinol Metab 2004;287:E340–E347. [PubMed: 15126238]
16. Olofsson J, Pihl J, Sinclair J, Sahlin E, Karlsson M, Orwar O. Anal Chem 2004;76:4968–4976. [PubMed: 15373430]

17. Sinclair J, Pihl J, Olofsson J, Karlsson M, Jardemark K, Chiu DT, Orwar O. Anal Chem 2002;74:6133–6138. [PubMed: 12510730]
18. Olofsson J, Bridle H, Sinclair J, Granfeldt D, Sahlin E, Orwar O. Proc Natl Acad Sci USA 2005;102:8097–8102. [PubMed: 15928088]
19. Lee PJ, Gaige TA, Hung PJ. Lab Chip 2009;9:164–166. [PubMed: 19209350]
20. Bennett MR, Pang WL, Ostroff NA, Baumgartner BL, Nayak S, Tsimring LS, Hasty J. Nature 2008;454:1119–1122. [PubMed: 18668041]
21. Azizi F, Mastrangelo CH. Lab Chip 2008;8:907–912. [PubMed: 18497910]
22. Xie Y, Wang Y, Chen L, Mastrangelo CH. Lab Chip 2008;8:779–785. [PubMed: 18432349]
23. Zhang XY, Roper MG. Anal Chem 2009;81:1162–1168. [PubMed: 19178342]
24. Hartmann DM, Nevill JT, Wyrick D, Votaw GA, Crenshaw HC. Lab Chip 2009;9:2332–2338. [PubMed: 19636464]
25. Wunderlich BK, Klessinger UA, Bausch AR. Lab Chip 2010;10:1025–1029. [PubMed: 20358110]
26. Grynkiewicz G, Poenie M, Tsien RY. J Biol Chem 1985;260:3440–3450. [PubMed: 3838314]
27. Ainla A, Gozen I, Orwar O, Jesorka A. Anal Chem 2009;81:5549–5556. [PubMed: 19476370]
28. Grover WH, Skelley AM, Liu CN, Lagally ET, Mathies RA. Sens Actuators B 2003;89:315–323.
29. Longsworth LG. J Am Chem Soc 1953;75:5705–5709.
30. Grover WH, von Muhlen MG, Manalis SR. Lab Chip 2008;8:913–918. [PubMed: 18497911]
31. Unger MA, Chou HP, Thorsen T, Scherer A, Quake SR. Science 2000;288:113–116. [PubMed: 10753110]
32. Bridle H, Olofsson J, Jesorka A, Orwar O. Anal Chem 2007;79:9286–9293. [PubMed: 18001008]
33. Tornheim K. Diabetes 1997;46:1375–1380. [PubMed: 9287034]
34. Bertram R, Sherman A, Satin LS. Am J Physiol Endocrinol Metab 2007;293:E890–E900. [PubMed: 17666486]
35. Bergsten P. Diabetes Met Res Rev 2000;16:179–191.
36. Hellman B, Gylfe E, Bergsten P, Grapengiesser E, Lund PE, Berts A, Dryselius S, Tengholm A, Liu YJ, Eberhardson M, Chow RH. Diabete Metab 1994;20:123–131. [PubMed: 7805949]
37. Gilon P, Ravier MA, Jonas JC, Henquin JC. Diabetes 2002;51:S144–S151. [PubMed: 11815474]
38. Bennett MR, Hasty J. Nat Rev Genet 2009;10:628–638. [PubMed: 19668248]
39. Kuczenski B, Ruder WC, Messner WC, LeDuc PR. PLoS ONE 2009;4:e4847. [PubMed: 19287482]

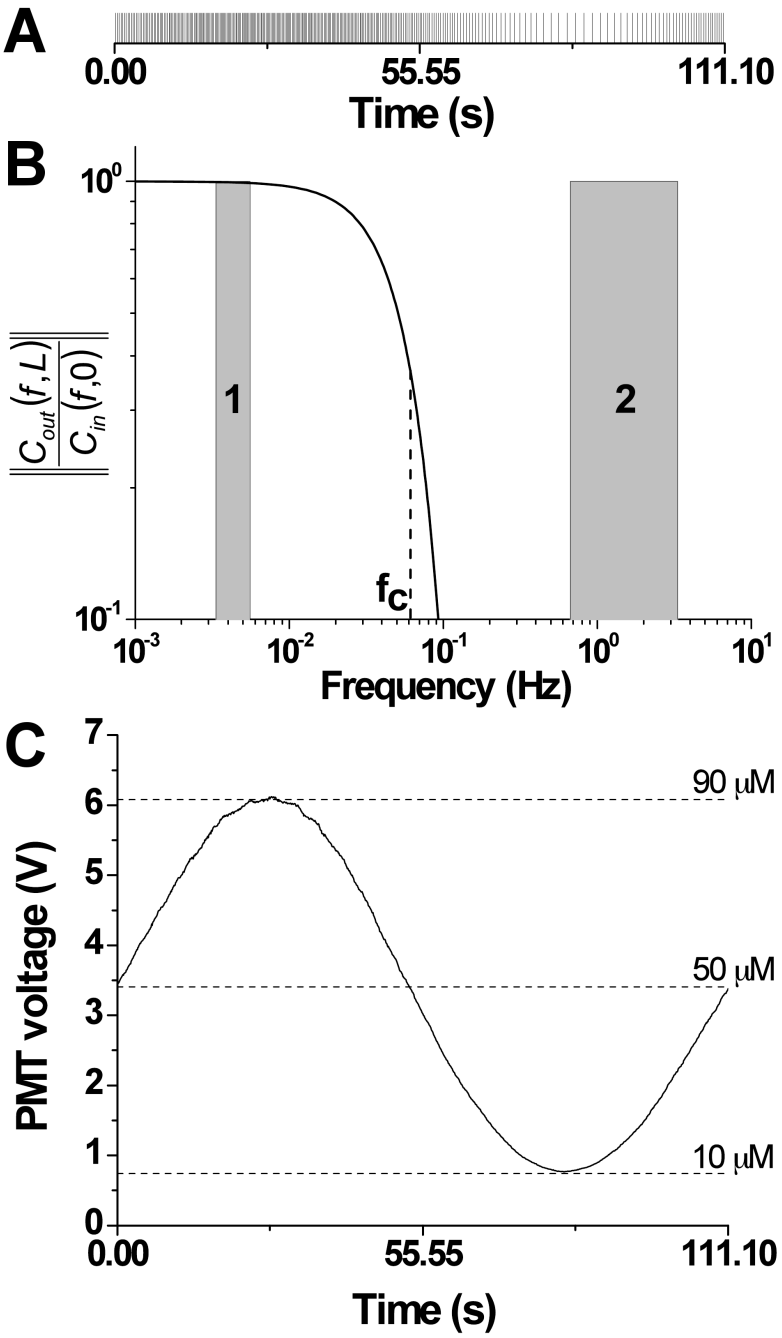

Figure 1. The low pass effect of the mixing channel to analyte pulses

A. Pulses of fluorescein were delivered to the mixing channel at the times specified by the vertical lines. The pulses were delivered at an average frequency of 3.33 Hz with the final concentration of the pulses dictated by the density of the pulses. **B.** Using the optimum channel dimensions and pumping parameters found in this report, the attenuation of output waveforms as a function of input frequency was modeled with equation 1 using a cutoff frequency (f_C) of 0.061 Hz. The two shaded regions indicate the frequencies used to entrain islets (shaded region 1) and the pumping frequencies (shaded region 2). **C.** After passing the high frequency pulses shown in **A** through the microfluidic device with the filter

characteristics shown in **B**, the output was a 0.009 Hz sine wave with an amplitude of 40 μM.

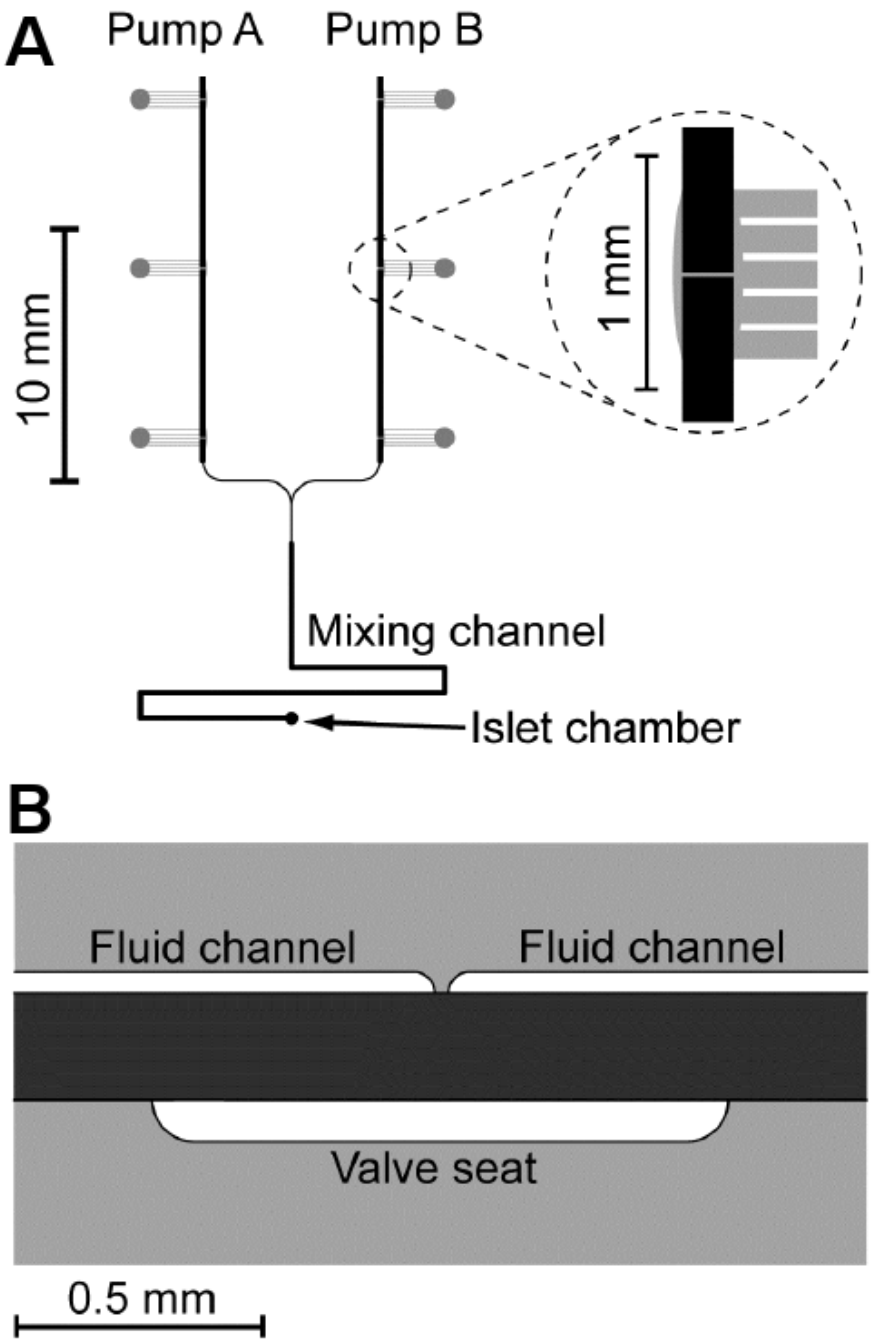

Figure 2. Microfluidic chip and valve design for high pumping frequency

A. Top view of the layout for the microfluidic device used in this report. Pump A and B delivered analyte and solvent pulses, respectively, into the mixing channel while maintaining a total flow rate of 1.5 ± 0.1 μL/min. A zoomed in view of one of the valves is shown in the inset. Pneumatic channels are shown in grey and fabricated in the bottom glass layer of the 3-layer device. Fluidic channels are shown in black and fabricated in the top glass layer. **B.** Side view of a valve used for rapid pumping. The contact area of glass-PDMS was minimized in the closed and open states by minimizing the distance between the fluid channels and deepening the valve seat, respectively.

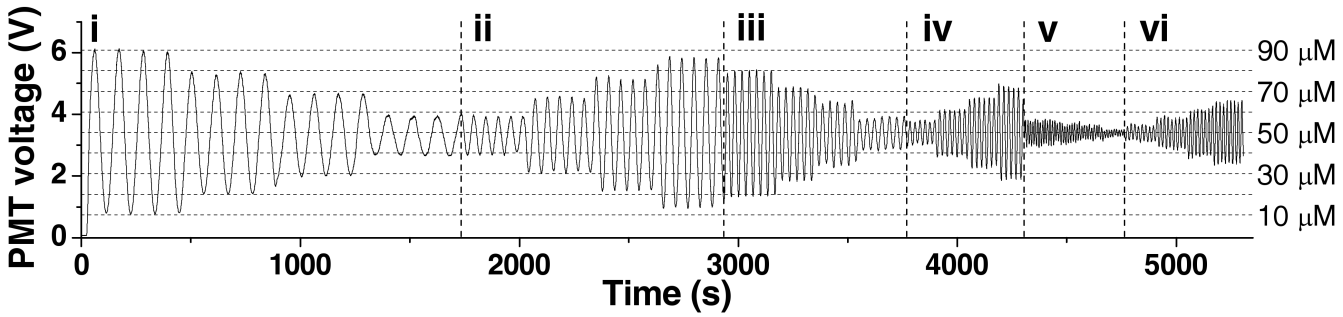

Figure 3. Fluorescein waveforms

From left to right, the input frequencies and amplitudes of sine waves were: (i) 0.009 Hz, from 40 μM to 10 μM, (ii) 0.018 Hz, from 10 μM to 40 μM, (iii) 0.030 Hz, from 40 μM to 10 μM, (iv) 0.045 Hz, from 10 μM to 40 μM, (v) 0.090 Hz, from 40 μM to 10 μM, and (vi) 0.060 Hz, from 10 μM to 40 μM. The amplitudes were compared to the intensities of an online dilution of fluorescein from 10 – 90 μM which are shown as the horizontal dashed lines.

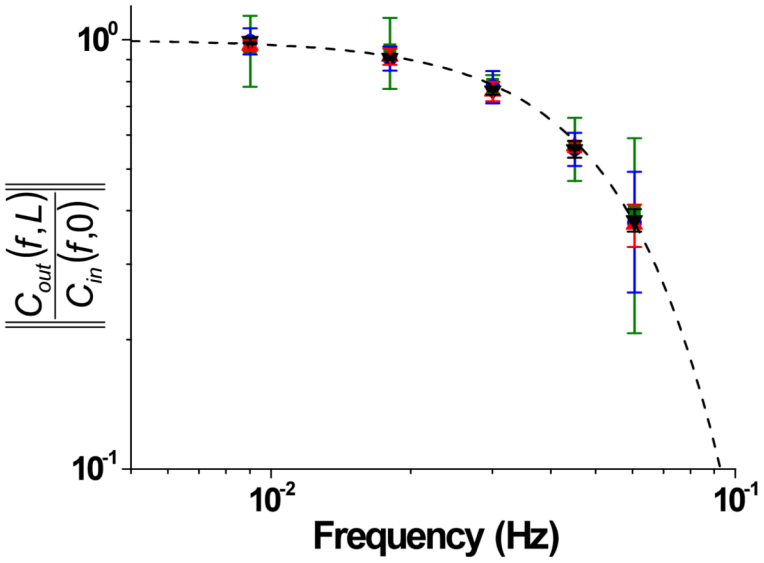

Figure 4. Attenuation of sine waves

Sine waves with amplitudes of 40 μM (black triangle, ▼), 30 μM (red triangle, ▲), 20 μM (blue circle, ●), and 10 μM (green square, ■) were applied with periods of 0.009 Hz, 0.018 Hz, 0.030 Hz, 0.045 Hz, 0.060 Hz and the attenuation of the output waveforms were determined as described in the text. The dashed line was found from Equation 1 using f_C = 0.061 Hz.

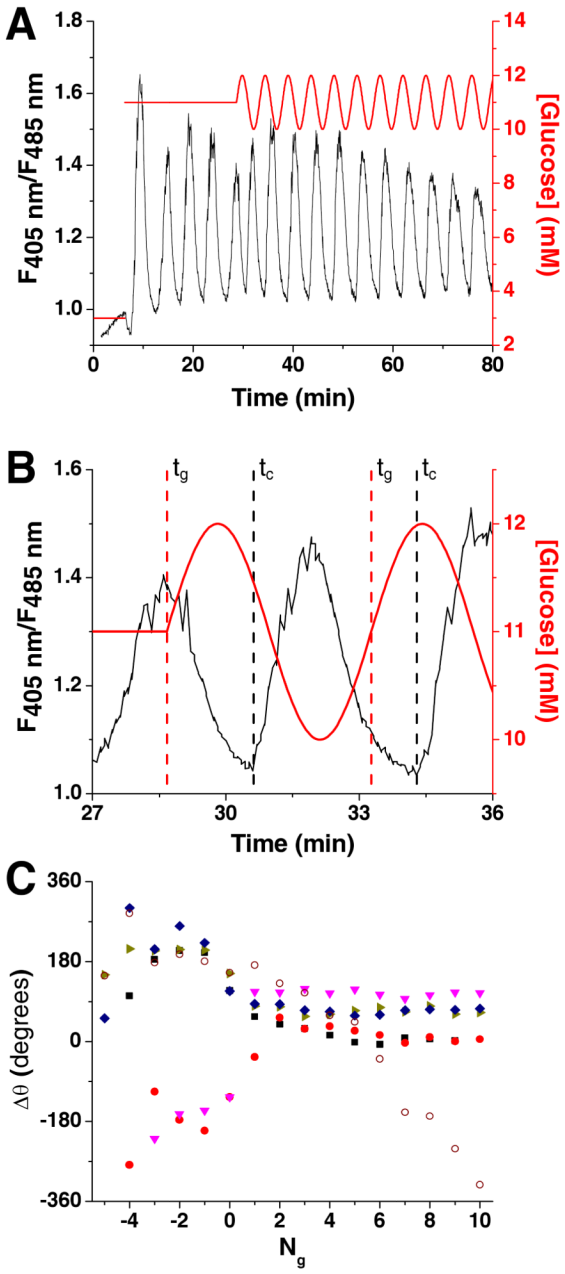

Figure 5. Oscillatory glucose concentrations applied to islets of Langerhans

A. Glucose (red line) was raised from 3 to 11 mM to induce oscillations in $[Ca^{2+}]_i$ (black line) from single islets of Langerhans. The glucose concentration was then made to oscillate about a mean of 11 mM, with amplitude of 1 mM and frequency comparable to the natural oscillations of $[Ca^{2+}]_i$. **B.** The $[Ca^{2+}]_i$ trace from Figure 5A is zoomed in on the first two glucose waves. Shown are the times corresponding to the start of the glucose waves (t_g) and $[Ca^{2+}]_i$ oscillations (t_C) where the difference in these times are proportional to the phase offset ($\Delta\theta$) shown in Figure 5C. **C.** The $\Delta\theta$ between the onset of each $[Ca^{2+}]_i$ oscillation and glucose wave was plotted as a function of the number of glucose waves applied (N_g). The glucose waves were started at $N_g = 0$ with negative values corresponding to $[Ca^{2+}]_i$ oscillations that occurred prior to the onset of the sinusoidal glucose waveform. Included is a

representative trace from an islet that was exposed to a constant 11 mM glucose (O) where Δθ did not stabilize and varied throughout the experiment.

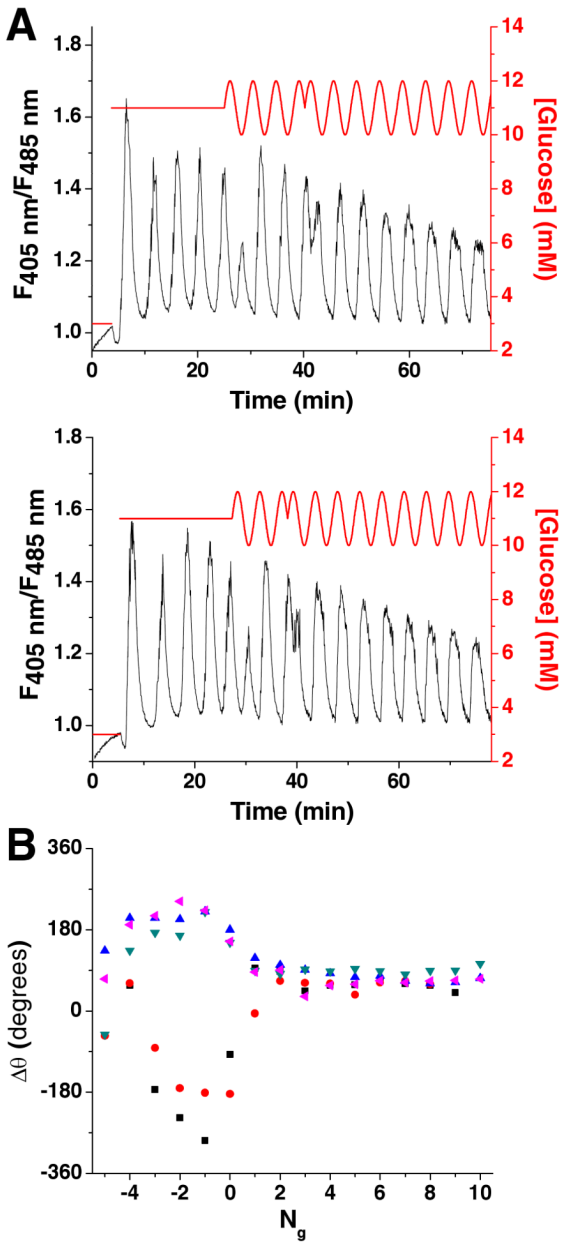

Figure 6. 180-degree glucose phase shifts

A. Two representative traces of the $[Ca^{2+}]_i$ changes that occurred when a 180° phase shift was introduced to the sinusoidal glucose waveform. The $[Ca^{2+}]_i$ oscillation that was affected by the glucose phase shift was much wider than adjacent $[Ca^{2+}]_i$ oscillations. **B.** For all islets tested, there was no change in Δθ after the 180° glucose phase shift, indicating that the islet quickly reset to the new glucose waves.